Magnetic susceptibility due to disorder-induced neutral solitons in interacting polymer chains

Marc Thilo Figge, Maxim Mostovoy, and Jasper Knoester
Institute for Theoretical Physics and Materials Science Center, University of Groningen, Nijenborgh 4, 9747 AG Groningen, The Netherlands
(Received 16 November 1998)

We study the magnetic response due to neutral solitons induced by disorder in polymer materials. We account for interchain interactions, which, if sufficiently strong, result in a bond-ordered phase, in which the neutral solitons are bound into pairs. We analytically calculate the corresponding pair-size distribution. As the spins of the solitons have a distance-dependent antiferromagnetic coupling, this allows us to calculate the magnetic susceptibility in the ordered phase. At low temperatures, the result deviates from the usual Curie behavior in a way that depends on the relative strength of the disorder and the interchain interactions. We compare our results to the observed magnetic susceptibility of *trans*polyacetylene and we suggest experiments extending towards lower temperatures. [S0163-1829(99)02721-6]

I. INTRODUCTION

In recent papers we have studied the effect of off-diagonal disorder on the lattice configuration of a half-filled Peierls-Hubbard chain with a doubly degenerate ground state.[1,2] An example is the π-conjugated polymer *trans*polyacetylene, which in the absence of disorder has a uniformly dimerized ground state. As the energy does not depend on the sign of the lattice dimerization (which determines whether even or odd bonds are short), this ground state is doubly degenerate. For a single Peierls-Hubbard chain, we showed that arbitrarily weak off-diagonal disorder induces neutral solitons (kinks) in the lattice dimerization, which interpolate between the two degenerate bond alternations. Even though the creation energy of a neutral soliton is rather large (of the order of the gap in *trans*polyacetylene), the energy loss is compensated by allowing the sign of the dimerization to adjust to the electronic disorder fluctuations. Off-diagonal disorder in conjugated polymers (i.e., disorder in the hopping amplitudes of the π electrons) may originate from random chain twists, which decrease the overlap between the π orbitals of neighboring carbon atoms. The density of disorder-induced neutral solitons in a single chain is proportional to the disorder strength.[1,2]

In *trans*polyacetylene the disorder strength is presumably rather large, as the average conjugation length in this material is of the order of several tens of carbon atoms only.[3] One would then expect the neutral solitons to contribute significantly to the polymer's magnetic and optical properties, as they carry spin $\frac{1}{2}$ and result in the appearance of electronic states inside the Peierls gap.

There is, however, no direct evidence for the existence of a high density of solitons in undoped *trans*polyacetylene. Electron spin resonance (ESR) experiments report only about one free spin per 3000 carbon atoms.[4–7] Moreover, it appears difficult to observe neutral solitons in optical-absorption experiments, as, contrary to what is expected from the Su-Schrieffer-Heeger (SSH) model,[8] they seem not to give rise to a clear midgap absorption peak.[9] This may be explained by assuming that the on-site Coulomb repulsion U is strong enough to shift the midgap peak towards the absorption edge resulting from interband transitions.[10,11] Since both the peak and the absorption edge are significantly broadened by the quantum lattice motion,[12] there may be no clear distinction between them.

X-ray scattering data do yield some indirect evidence for disorder-induced kinks. There still is considerable disagreement whether neighboring carbon chains are dimerized in phase ($P2_1/a$ space group) or in antiphase ($P2_1/n$ space group).[13,14] While this may originate from different preparation methods leading to different space groups, it has also been pointed out that the disagreement may result from a high density (of the order of several percent) of kinks that locally change the relative sign of the dimerization in neighboring chains.[15,16] Yet, it is not clear how such random changes would lead to sharp peaks in the x-ray spectra.

From the above it appears that a clear signature of the effect of disorder-induced solitons is still to be found. This has motivated us to study the magnetic response of disorder-induced solitons in more detail. A proper modeling of the magnetic susceptibility involves more than a calculation of the density of solitons in an isolated chain. As we noted in Refs. 1 and 2, the actual density of neutral solitons (and thus of spins) is determined by the competition between disorder and interchain interactions, as the latter lead to confinement of soliton-antisoliton pairs and may restore the long-range bond order. Moreover, at low temperature, the exchange between the spins of neighboring solitons on a single chain tends to bind them into a singlet state,[17] which has no magnetic response. Thus, the magnetic susceptibility and, in particular, its temperature dependence should be expected to depend strongly on the interplay between disorder and interchain interactions.

In this paper, we focus on the magnetic susceptibility of disorder-induced solitons in the phase with long-range bond order. In this case, solitons occur in isolated pairs of random size dictated by the disorder realization. We study the statistics of these pairs by mapping the problem on the anisotropic random-field Ising model, which is treated in the chain-mean-field approximation.[18] This mapping is analogous to what we did in Refs. 1 and 2 for isolated chains. We briefly explain the mapping in Sec. II and discuss the phase diagram

of this model. In Sec. III, we express the magnetic susceptibility of an ensemble of soliton-antisoliton pairs in terms of the, as yet unknown, distribution of exchange interactions. In Sec. IV, we calculate the distribution of soliton-pair sizes using the saddle-point method. From the pair-size distribution we derive in Sec. V the distribution of exchange constants. The latter is used in Sec. VI to calculate the magnetic susceptibility of *trans*polyacetylene. We find that the low-temperature behavior of this susceptibility deviates from the Curie law and we fit our results to the experimental data obtained in Ref. 7. In Sec. VII, we summarize and conclude.

II. SOLITONS IN INTERACTING DISORDERED PEIERLS CHAINS

In Ref. 2, we have shown that the statistics of neutral solitons in isolated weakly disordered Peierls chains can be studied using the one-dimensional random-field Ising model (RFIM). In this mapping, Ising variables $\sigma_m = \pm 1$ ($m = 1, \ldots, M$) are defined on the sites of a lattice with lattice constant d. These variables play the role of the sign of the dimerization in the Peierls chain, while the random ''magnetic'' field h_m at site m represents the off-diagonal disorder, which locally lifts the degeneracy between the two dimerization phases in the Peierls chain. Two neighboring sites on the lattice having different Ising variable, correspond to the occurrence of a soliton in the Peierls chain. Therefore, the creation energy μ of a soliton in the Peierls chain is equivalent to the exchange interaction between neighboring Ising spins. In the SSH model of *trans*polyacetylene $\mu = 2\Delta_0/\pi \simeq 0.5$ eV (Δ_0 is the dimerization). We emphasize, however, that this mapping is not limited to the SSH model, but also holds in the presence of electron-electron interactions, in which case the value of μ is smaller.[19,20]

Our approach may easily be extended to account for three-dimensional effects: interchain interactions (electron hopping, elastic forces, or Coulomb interactions) tend to favor a coherence of the dimerization pattern on neighboring chains, which in Ising language translates into an interaction $2W$ between spins or neighboring chains. As for quasi-one-dimensional materials, like conjugated polymers, $W \ll \mu$, we are thus dealing with a strongly anisotropic random-field Ising model.[18] The anisotropy allows one to treat the interchain interactions in a mean-field way, an approach known as the chain-mean-field approximation. The energy of the resulting Ising model is given by

$$E\{\sigma_m\} = \sum_{m=1}^{M} \left[\frac{\mu}{2}(1 - \sigma_m \sigma_{m+1}) - h_m \sigma_m - B\sigma_m \right]. \quad (1)$$

Here, the first term describes the energy cost for creating $\frac{1}{2}\sum_{m=1}^{M}(1-\sigma_m\sigma_{m+1})$ kinks and the second term describes the interaction energy with the random-magnetic field. The latter is assumed to have a Gaussian distribution with zero mean ($\langle h_m \rangle = 0$) and correlator

$$\langle h_m h_n \rangle = \epsilon \delta_{m,n}, \quad (2)$$

where ϵ is the disorder strength. We consider the case of weak disorder: $\epsilon \ll \mu^2$. Finally, the third term in Eq. (1) describes the interchain interactions in the mean-field approximation, where the homogeneous ''magnetic'' field B is proportional to the average order parameter

$$B = W\langle\langle \sigma \rangle\rangle. \quad (3)$$

The double brackets denote both the thermal and the random-field average.

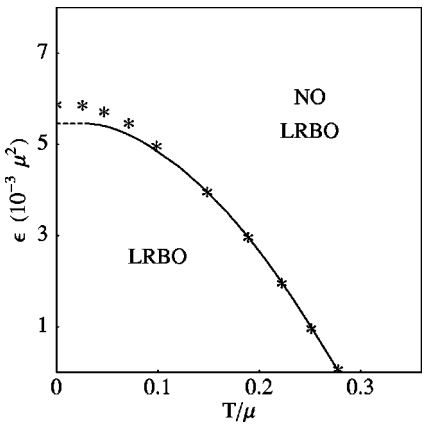

FIG. 1. The phase diagram of the RFIM Eq. (1) captures the essential physics of weakly disordered Peierls systems and is shown as a function of the disorder strength ϵ/μ^2 and the temperature T/μ. The long-range bond order (LRBO) phase corresponds to an average dimerization $\langle\langle \sigma \rangle\rangle \Delta_0 \neq 0$. The numerical calculation of the critical curve (stars) agrees well with the analytical result (solid curve) obtained in Ref. 18. The dashed curve indicates the breakdown of the continuum approximation in the analytical calculation below $T = T_0(\epsilon)$ (Ref. 18).

To end the explanation of our model, a few remarks are in place. First, by replacing the dimerization by a discrete Ising variable, we have neglected the true dimerization profile associated with a soliton. As the extent of this profile is given by the correlation length ξ_0, our ''sudden-kink approximation'' is valid as long as the soliton density is small compared to $1/\xi_0$, as is the case for weak disorder. Taking into account the true dimerization profile results in an effective increase of the kink creation energy of the order $\sqrt{\epsilon \xi_0 / a}$ (with a the average carbon-carbon distance in *trans*polyacetylene) and, thus, in a small reduction of the soliton density. This has recently been confirmed explicitly in numerical simulations, which do account for the true profile.[21] Second, it should be kept in mind that the RFIM Eq. (1) is an effective model, obtained by integrating out small lattice fluctuations. As a result, the kink creation energy μ weakly depends on the temperature.[2] Third, above we have not specified the value of the Ising lattice constant d (which should not be confused with the lattice constant a of the polymer chain). It should be noted that both the disorder strength ϵ and the interchain interaction energy W scale proportional to d. In Sec. V, we show that all physical observables are d independent in the $d \to 0$ limit.

The temperature versus disorder strength phase diagram of the model Eq. (1) contains two phases: the ordered phase characterized by a nonzero value of the average dimerization, $\langle\langle \sigma \rangle\rangle \Delta_0$, and the disordered phase, in which the long-range bond order (LRBO) is destroyed by thermal and disorder-induced kinks. The two phases are separated by a second-order transition. Figure 1 shows the phase diagram

calculated for $W/\mu=0.008$, a typical value of *trans*polyacetylene if the interchain interactions are dominated by interchain electron hopping.[22] The stars in Fig. 1 denote the phase boundary, which we obtained by numerical simulation of the model Eq. (1) using an algorithm based on the transfer-matrix approach (cf. Ref. 2). The order parameter $\langle\langle\sigma\rangle\rangle$ was found from a self-consistent calculation of the mean field B and the critical curve was then obtained by requiring that $\langle\langle\sigma\rangle\rangle\to 0$. The smooth temperature dependence of the phase boundary was obtained by averaging the free energy over 10^4 random-field realizations for a chain with 10^3 sites. The solid curve in Fig. 1 indicates the phase boundary, which was calculated in Ref. 18 from an analytical expression for the average free energy of the continuum version of the model Eq. (1). With the exception of a small temperature region $T<T_0(\epsilon)$,[18] the results of the continuum and the discrete models agree well.

At low temperature, the phase transition results from a competition between the disorder and the interchain interactions. In fact, the critical disorder strength, which separates the phases with and without LRBO at zero temperature reads[18]

$$\epsilon_c \approx \frac{2}{3} W\mu. \tag{4}$$

In the disordered phase, $\langle\langle\sigma\rangle\rangle=0$, the density of disordered-induced neutral solitons (spin flips) is to lowest order in ϵ given by[18]

$$n_s=\frac{1}{d}\frac{\epsilon}{\mu^2}, \tag{5}$$

as is the case for a single disordered chain ($W=0$).[23] On the other hand, for $\epsilon<\epsilon_c$ the order parameter $\langle\langle\sigma\rangle\rangle$ is observed to increase rapidly[18] with a slope that is proportional to the ratio $\mu/W\gg 1$. Thus, in the overwhelming part of the ordered phase the system is nearly perfectly ordered with an order parameter close to unity, $\langle\langle\sigma\rangle\rangle\simeq 1$, and the solitons are bound into pairs by the interchain interactions. Well within the ordered phase ($\epsilon\ll\epsilon_c$) their density is exponentially suppressed. The distance between the soliton-antisoliton pairs is much larger than the typical pair size and the number of soliton-antisoliton pairs per unit length reads[18]

$$n_p=\frac{1}{d}\frac{2W^2}{\epsilon}\exp\left(-2\frac{W\mu}{\epsilon}\right) \tag{6}$$

(for $W^2\ll\epsilon\ll 2W\mu/3$).

In the following, we will focus on the LRBO phase and calculate the magnetic susceptibility due to the spins of the bound pairs of neutral solitons.

III. MAGNETIC SUSCEPTIBILITY IN THE ORDERED PHASE

Apart from the interchain interaction discussed in the previous section, there is also an intrachain interaction between kinks. The latter interaction is strong only when the distance between kinks is of the order of their size, ξ_0. Thus, for weak disorder, when the density of kinks is small, it has little effect on the statistics of the kinks. It may, however, be important for the magnetic properties of disordered Peierls systems, as it results in an antiferromagnetic exchange between the spins of neutral kinks.[17] This exchange can bind the spins of neighboring kinks into nonmagnetic singlets, thus reducing the magnetic susceptibility of the system.

As argued in the previous section, for a nearly perfectly ordered system the typical distance between disorder-induced soliton-antisoliton pairs is much larger than the typical pair size. We may then neglect the spin exchange between kinks from different pairs. The Hamiltonian describing the interactions of soliton and antisoliton spins $\vec{S}_1$ and $\vec{S}_2$ within one pair reads

$$\hat{H}_{\rm pair}=J(\vec{S}_1\cdot\vec{S}_2-\tfrac{1}{4})-g\mu_B H(S_1^z+S_2^z), \tag{7}$$

where J is the exchange constant in the pair and H is the external magnetic field. The free energy of the pair is given by

$$f(J,H)=-J-\frac{1}{\beta}\ln\{1+e^{-\beta J}[1+2\cosh(\beta g\mu_B H)]\} \tag{8}$$

and the zero-field magnetic susceptibility of the pair is

$$\chi(T,J)=-\left.\frac{\partial^2 f(J,H)}{\partial H^2}\right|_{H=0}=2g^2\mu_B^2\beta\frac{e^{-\beta J}}{1+3e^{-\beta J}}. \tag{9}$$

The coupling J decreases with the soliton-antisoliton separation R. Quite generally, the large-R behavior is

$$J=J_0\exp\left(-\frac{R}{\rho}\right), \tag{10}$$

where $\rho=\xi_0/d$ (R is measured in units of d) and J_0 is of the order of the spin gap. For the SSH model, in which Coulomb interactions are neglected and the spin gap equals the charge gap, $J_0=4\Delta_0$.[17]

As R is a random quantity that is imposed by the disorder realization, also J is random. If we know the pair-size distribution $p(R)$ the distribution of exchange values $w(J)$ can be obtained using Eq. (10). We normalize the latter to the total density of spin pairs

$$n_p=\int_0^\infty dJ\, w(J). \tag{11}$$

The system's magnetic susceptibility is then given by

$$\chi(T)=\int_0^\infty dJ\, w(J)\chi(T,J), \tag{12}$$

with $\chi(T,J)$ as in Eq. (9).

Clearly, the temperature dependence of the magnetic susceptibility is determined by the pair-size distribution. As we will show in detail in Secs. IV and V, in the LRBO phase $p(R)$ is sharply peaked at some R^*, while for $R\gg R^*$

$$p(R\gg R^*)\propto\exp\left(-\alpha\frac{R}{\rho}\right) \tag{13}$$

with α a constant determined by the strength of the disorder and interchain interactions. Equation (13) in a straightforward way yields a power-law exchange distribution

$$w(J)\propto\left(\frac{J_0}{J}\right)^{1-\alpha} \tag{14}$$

for $J\ll J(R^*)$. This part of $w(J)$ dictates the behavior of the magnetic susceptibility at low temperature, $T\ll J(R^*)$. Pairs with $J\gg J(R^*)$ (or: $R\ll R^*$) are in the nonmagnetic singlet state at these low temperatures. We thus find

$$\chi[T\ll J(R^*)]\propto\left(\frac{J_0}{T}\right)^{1-\alpha}, \tag{15}$$

which deviates from the high-temperature Curie behavior.

We note that, in order to describe the anomalous temperature dependence of the magnetic susceptibility of charge-transfer salts, Clark *et al.*[24] also introduced pairs of spins with a random antiferromagnetic coupling. These pairs, however, were introduced in a purely phenomenological way, whereas in our model they naturally emerge as disorder-induced soliton-antisoliton pairs with a distribution of exchange constants that follows from the pair-size distribution.

IV. CALCULATION OF THE PAIR-SIZE DISTRIBUTION

The pair-size distribution $p(R)$ is defined as the number of soliton-antisoliton pairs of size R per site of the Ising chain. For a given disorder realization $\{h_m\}$ one finds from Eq. (1) that the energy of a configuration (m_1,m_2), with the soliton located between m_1 and m_1+1 and the antisoliton between m_2 and m_2+1, reads

$$E[m_1,m_2]=E_0-\Delta E[m_1,m_2], \tag{16}$$

where E_0 denotes the energy for a configuration without solitons and

$$\Delta E[m_1,m_2]=-2\mu-2\sum_{m=m_1+1}^{m_2}(B+h_m) \tag{17}$$

is the energy change due to the creation of the soliton-antisoliton pair. As we restrict ourselves to isolated soliton-antisoliton pairs, it is sufficient to consider a segment of the chain that contains one such pair located far away from its endpoints. Furthermore, because the sequence of solitons and antisolitons along the chain is determined by fixed boundary conditions for the lattice dimerization, we may, without loss of generality, assume that $m_2>m_1$. Then, the pair size R (in units of the Ising lattice constant d) is given by

$$R=m_2-m_1. \tag{18}$$

The soliton-antisoliton pair configuration (m_1,m_2) is only energetically favorable if

$$\Delta E[m_1,m_2]\geqslant 0. \tag{19}$$

This is, however, not sufficient to calculate the pair-size distribution $p(R)$, as we also have to impose the condition that this pair configuration has lower energy than any other pair in the considered chain segment. Thus, simultaneously, the energy of the pair configuration has to satisfy the inequalities

$$\Delta E[m_1,m_2]\geqslant\Delta E[m_1',m_2'], \tag{20}$$

for all other possible pair configurations (m_1',m_2'). Therefore, the desired pair-size distribution takes the form:

$$p(R)=\left\langle\Theta(\Delta E[m_1,m_2])\prod_{(m_1',m_2')}\Theta(\Delta E[m_1,m_2]-\Delta E[m_1',m_2'])\right\rangle, \tag{21}$$

where $\Theta(x)$ is the step function

$$\Theta(x)=\begin{cases}1 & \text{for } x\geqslant 0\\ 0 & \text{for } x<0\end{cases} \tag{22}$$

and the brackets, $\langle\ldots\rangle$, denote the Gaussian average over disorder realizations $\{h_m\}$. The definition Eq. (21) ensures that, in accordance with Eq. (11), $p(R)/d$ is normalized to the density of soliton-antisoliton pairs

$$n_p=\frac{1}{d}\int_0^\infty dR\,p(R). \tag{23}$$

It is easy to see that $p(R)$ factorizes into two independent parts, $p_{\rm out}$ and $p_{\rm in}$, that account for the soliton-antisoliton pairs with a size that is, respectively, larger and smaller than R

$$p(R)=p_{\rm out}p_{\rm in}, \tag{24}$$

with

$$\begin{aligned}p_{\rm out}=&\langle\Theta(z+s_{m_1})\Theta(2z+s_{m_1}+s_{m_1-1})\\&\times\Theta(3z+s_{m_1}+s_{m_1-1}+s_{m_1-2})\ldots\rangle\\&\times\langle\Theta(z+s_{m_2+1})\Theta(2z+s_{m_2+1}+s_{m_2+2})\\&\times\Theta(3z+s_{m_2+1}+s_{m_2+2}+s_{m_2+3})\ldots\rangle,\end{aligned} \tag{25}$$

and

$$p_{\rm in}=\left\langle\Theta\left(-I-Rz-\sum_{m=m_1+1}^{m_2}s_m\right)\Pi_L\Pi_R\right\rangle. \tag{26}$$

Here, we have defined the dimensionless variables $s_m=h_m/\sqrt{\epsilon}$, $z=B/\sqrt{\epsilon}$, $I=\mu/\sqrt{\epsilon}$, while

$$\begin{aligned}\Pi_L\equiv&\Theta(-z-s_{m+1})\Theta(-2z-s_{m_1+1}-s_{m_1+2})\ldots\\&\times\Theta(-Rz-s_{m_1+1}-\ldots-s_{m_2})\end{aligned} \tag{27}$$

and

$$\begin{aligned}\Pi_R\equiv&\Theta(-z-s_{m_2})\Theta(-2z-s_{m_2}-s_{m_2-1})\ldots\\&\times\Theta(-Rz-s_{m_2}-\ldots-s_{m_1+1}).\end{aligned} \tag{28}$$

Note that $p_{\rm out}$ itself also consists of two independent factors: the first factor excludes the pairs with the soliton located to the left of m_1, while the second one excludes antisoliton positions larger than m_2+1. Both these factors can be written in the form

$$Y(z)=\prod_{m=1}^{\infty}\left\{\int_{-\infty}^{+\infty}ds_m f(s_m)\Theta\left[\sum_{k=1}^{m}(z+s_k)\right]\right\}, \quad (29)$$

where

$$f(s)=\frac{\exp(-\frac{1}{2}s^2)}{\sqrt{2\pi}} \quad (30)$$

is the Gaussian weight. As a result, for the outer factor we obtain

$$p_{\rm out}=[Y(z)]^2. \quad (31)$$

The function $Y(z)$ will be calculated later in this section.

The calculation of the inner factor is complicated by the presence of the extra Θ function in Eq. (26), which precludes the factorization of $p_{\rm in}$ in two independent averages. However, considerable simplification is possible, because we focus on the bond-ordered phase where $\langle\langle\sigma\rangle\rangle\simeq 1$. Then the density of disorder-induced soliton-antisoliton pairs is small, and the main suppression factor in $p(R)$ is the probability of the disorder realization necessary to create a pair.[25,26] In other words, the most important contribution to $p_{\rm in}$ [and $p(R)$] comes from averaging the first Θ function in Eq. (26)

$$\left\langle\Theta\left[-I-\sum_{m=m_1+1}^{m_2}(z+s_m)\right]\right\rangle=\frac{1}{2}\mathrm{erfc}[g(R)] \approx\frac{\exp[-g(R)^2]}{\sqrt{4\pi}g(R)}, \quad (32)$$

where

$$g(R)\equiv\frac{I+Rz}{\sqrt{2R}}. \quad (33)$$

Here, the asymptotic expression for the complementary error function $\mathrm{erfc}[g(R)]$ was used because the minimal value for its argument is easily shown to be $g_{\min}=\sqrt{3\epsilon_c/\epsilon}$, so that for $\epsilon\leqslant\epsilon_c/2$ the relative error becomes already less than several percent.

The interpretation of this result is that the optimal disorder fluctuation (i.e., the disorder realization with the largest weight) that can induce a soliton-antisoliton pair of size R has a constant value $-h_R$ in the interval of length R and is zero outside the interval. The amplitude h_R is determined by the energy balance [see Eqs. (17) and (19)]

$$h_R R=\mu+WR. \quad (34)$$

The weight of the optimal fluctuation, $w=\exp[-Rh_R^2/(2\epsilon)]$, is precisely the exponential factor appearing in Eq. (32). At

$$R^*=\frac{I}{z}=\frac{\mu}{W}\gg 1 \quad (35)$$

the weight reaches its maximal value, $\exp(-2W\mu/\epsilon)$. For $\epsilon\ll\epsilon_c$, the maximal weight is small [as was also found in Eqs. (32) and (33)] and the soliton-antisoliton pairs are suppressed. In that case, all disorder realizations that contribute significantly to $p(R)$ are close to the optimal fluctuation.

Bearing this in mind, we now calculate the inner factor Eq. (26). First, we can rewrite Eq. (26) in the form

$$p_{\rm in}=\int_{zR+I}^{\infty}dS\int_{-i\infty}^{+i\infty}\frac{d\lambda}{2\pi i}e^{-\lambda S} \times\prod_{m=m_1+1}^{m_2}\int_{-\infty}^{+\infty}ds_m e^{-\lambda s_m}f(s_m)\Pi_L\Pi_R, \quad (36)$$

where the integration over λ ensures that

$$S=-\sum_{m=m_1+1}^{m=m_2}s_m \quad (37)$$

and the limits of the integration over S follows from the first Θ function in Eq. (26).

Since the typical pair size $R^*\gg 1$ [see Eq. (35)], we can use the canonical formalism, in which Eq. (37) for the sum of R random variables is satisfied only in average. We do this by ''shifting'' the argument of the random-field distribution on each site by λ

$$f(s)\to f(s+\lambda)=e^{-\frac{1}{2}\lambda^2-\lambda s}f(s), \quad (38)$$

so that the average value now becomes $s=-\lambda$ and Eq. (36) reads

$$p_{\rm in}=\int_{zR+I}^{\infty}dS\int_{-i\infty}^{+i\infty}\frac{d\lambda}{2\pi i}e^{-\lambda S+\frac{1}{2}R\lambda^2} \times\prod_{m=m_1+1}^{m_2}\int_{-\infty}^{+\infty}ds_m f(s_m+\lambda)\Pi_L\Pi_R. \quad (39)$$

The integral over λ comes from the small vicinity ($\sim 1/\sqrt{R}$) of $\lambda_0=S/R$, where the exponential in Eq. (39) has its maximum. Saddle-point integration over λ then gives

$$p_{\rm in}=\int_{zR+I}^{\infty}\frac{dS}{\sqrt{2\pi R}}e^{-\frac{S^2}{2R}}\prod_{m=m_1+1}^{m_2}\int_{-\infty}^{+\infty}ds_m f\left(s_m+\frac{S}{R}\right)\Pi_L\Pi_R. \quad (40)$$

Next, we note that if the condition imposed by the first Θ function in Eq. (26) is satisfied, the arguments of the last Θ functions in Π_L and Π_R also almost certainly are positive. In other words, because the relevant disorder realizations are close to the optimal fluctuations, only the first few Θ functions in Π_L and Π_R are really restrictive. This implies that the disorder averages of Π_L and Π_R in Eq. (40) are decoupled. Furthermore, it is easily seen from Eq. (29) that then $\langle\Pi_L\rangle=\langle\Pi_R\rangle=Y[(S/R)-z]$, so that Eq. (40) becomes

$$p_{\rm in}=\int_{zR+I}^{\infty}\frac{dS}{\sqrt{2\pi R}}e^{-(1/2R)S^2}\left[Y\left(\frac{S}{R}-z\right)\right]^2. \quad (41)$$

The integral over S comes from the vicinity of the lower limit, $S=zR+I$ [cf. Eq. (34) for the optimal fluctuation]. The result of the integration is

$$p_{\rm in}=\sqrt{\frac{R}{2\pi}}\frac{\exp\left[-\frac{(I+Rz)^2}{2R}\right]}{(I+Rz)}\left[Y\left(\frac{I}{R}\right)\right]^2, \quad (42)$$

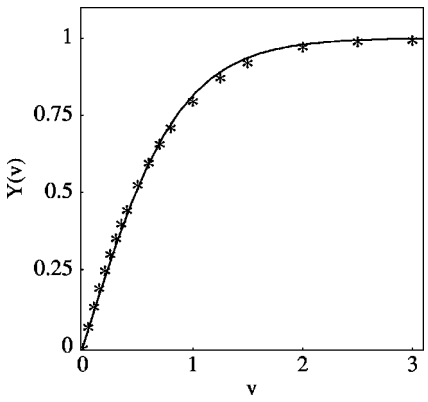

FIG. 2. The function $Y(v)$ obtained from a numerical solution (stars) of the integral equation (44). The best fit of this solution by a function of the form $Y(v)=\tanh(cv)$ yields $c\simeq 1.14$ (solid line).

where for S in the argument of Y we took its value at the lower limit of the integration.

From Eqs. (24), (31), and (42) we finally obtain for the pair-size distribution

$$p(R)=\frac{\exp[-g(R)^2]}{\sqrt{4\pi}g(R)}\left[Y\left(\frac{I}{R}\right)\right]^2[Y(z)]^2, \tag{43}$$

where the function $g(R)$ is defined by Eq. (33).

What is left now, is the calculation of the function $Y(v)$. To this end we introduce the function $Y(s|v)$, satisfying the integral equation

$$Y(s|v)=\int_0^\infty ds' f(s+v-s')Y(s'|v). \tag{44}$$

Comparing the iterative solution of this equation to Eq. (29), one finds

$$Y(v)=Y(0|v). \tag{45}$$

The integral equation (44) can be easily solved numerically. The result is shown as stars in Fig. 2. The solid line represents the best fit to these points by a function of the form

$$Y(v)=\tanh(cv). \tag{46}$$

The fit yields $c\simeq 1.14$. For small v, the best linear fit $[Y(v)=c'v]$ yields $c'\simeq\sqrt{2}$, with a precision of several percent.

We conclude this section by a brief analysis of the pair-size distribution Eq. (43). First, integrating $p(R)/d$ over R gives the density of soliton-antisoliton pairs [cf. Eq. (23)]. For $\epsilon\ll\epsilon_c$, the exponential factor in Eq. (43) has a sharp peak at R^* given by Eq. (35). Using $B\simeq W$, the saddle-point integration around the peak gives

$$n_p\approx\frac{1}{d}\frac{\epsilon}{2W^2}\left[Y\left(\frac{W}{\sqrt{\epsilon}}\right)\right]^4\exp\left(-2\frac{W\mu}{\epsilon}\right). \tag{47}$$

Furthermore, we note that knowledge of the pair-size distribution Eq. (43) allows us to derive the long- and short-range bond order parameter of the RFIM Eq. (1). For a dilute gas of soliton-antisoliton pairs it is sufficient to consider a chain segment of $N+1$ sites containing a single pair of size R

$$\sigma(m)=1-2\Theta(m-m_1)\Theta(m_2-m), \tag{48}$$

where m_1 and $m_2=m_1+R$ denote the positions of, respectively, the soliton and the antisoliton. Replacing summations by integrations, the LRBO parameter averaged over all possible pair sizes is easily calculated

$$\langle\langle\sigma\rangle\rangle=\int_0^\infty dR\,p(R)\int_{-\frac{N}{2}}^{+\frac{N}{2}}dm\,\sigma(m)=1-2\int_0^\infty dR\,p(R)R. \tag{49}$$

For a nearly perfectly ordered system, $\langle\langle\sigma\rangle\rangle\simeq 1$, we thus find from Eq. (49) the condition that the typical pair size R^* is much smaller than the typical number of sites $1/(dn_p)$ between soliton-antisoliton pairs. Similarly, we calculate the correlation function $\langle\langle\sigma(0)\sigma(l)\rangle\rangle$, which yields the sum of the square of the LRBO parameter Eq. (49),

$$\langle\langle\sigma\rangle\rangle^2\simeq 1-4\int_0^\infty dR\,p(R)R, \tag{50}$$

and the connected correlator

$$\langle\langle\sigma(0)\sigma(l)\rangle\rangle_c=4\int_0^\infty dR\,p(R+|l|)R. \tag{51}$$

The scale for the decay of short-range correlations is obviously set by the typical pair size R^*, as $\langle\langle\sigma(0)\sigma(l)\rangle\rangle_c\to 0$ for $|l|\gg R^*$.

V. THE EXCHANGE DISTRIBUTION IN THE CONTINUUM LIMIT

In the previous sections we described disordered Peierls systems using the effective RFIM Eq. (1). The values of the interchain interaction W and the disorder strength ϵ in this model are proportional to the length d, which we choose for the unit cell of the Ising chain and which plays the role of a short-distance cutoff. On the other hand, physical observables, such as the density of soliton-antisoliton pairs and the magnetic susceptibility, should not depend on d. Thus, before comparing our results to the experimental data on *trans*polyacetylene, we show that d drops out from the expressions for the observables in the $d\to 0$ limit.

To this end, we introduce as physically meaningful quantities the disorder strength $\bar{\epsilon}$ and the interchain interaction $\bar{W}$ per unit length

$$\epsilon=\bar{\epsilon}d, \tag{52}$$

and

$$W=\bar{W}d. \tag{53}$$

Furthermore, from now on we will work with the physical pair size $r=Rd$. In terms of these new variables, the arguments of both Y functions in Eq. (43) for the pair-size distribution are $\propto\sqrt{d}$. Therefore, for $d\to 0$, the arguments are small and we can use $Y(v)\simeq\sqrt{2}v$ [see below Eq. (45)], giving the pair-size distribution

$$\bar{p}(r)=4\frac{\mu^2\bar{W}^2}{\bar{\epsilon}^2r^2}\frac{\exp[-g(r)^2]}{\sqrt{4\pi}g(r)}, \tag{54}$$

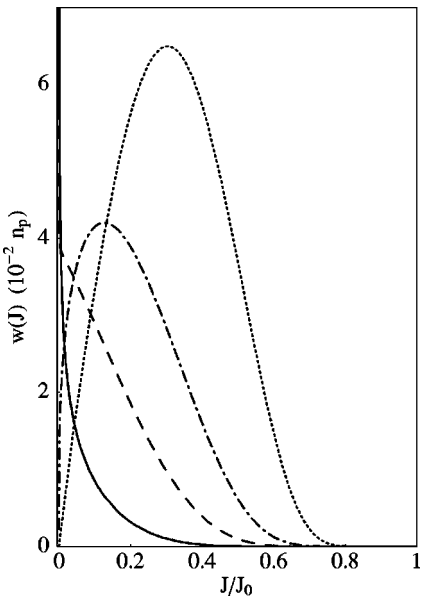

FIG. 3. The distribution $w(J)$ of exchange constants as a function of J/J_0 for the four parameter sets given in Table I. The curves correspond to $\alpha=1.5$ (dots), 1.0 (dash-dot), 0.75 (dashes), and 0.5 (solid). For $\alpha \geqslant 1.0$ the distribution has a pronounced peak at some $J=J^*$ and tends to zero for $J\to 0$. In contrast, for $\alpha<1.0$, $w(J)$ diverges when $J\to 0$.

where

$$g(r)=\frac{\mu+\overline{W}r}{\sqrt{2\overline{\epsilon}r}}. \tag{55}$$

Similarly, from Eq. (47), the total density of neutral soliton-antisoliton pairs in the limit $d\to 0$ is found to be

$$n_p \approx \frac{2\overline{W}^2}{\overline{\epsilon}}\exp\left(-2\frac{\overline{W}\mu}{\overline{\epsilon}}\right), \tag{56}$$

which coincides with Eq. (6) obtained in Ref. 18 within the continuum approximation for the RFIM Eq. (1).

Furthermore, in terms of continuum variables, the exchange coupling Eq. (10) reads

$$J(r)=J_0\exp\left(-\frac{r}{\xi_0}\right). \tag{57}$$

Thus, in the continuum limit the distribution of exchange constants becomes

$$w(J)=\int_0^\infty dr\,\overline{p}(r)\,\delta[J-J(r)]$$

$$=4\frac{1}{J}\frac{1}{\xi_0}\frac{\mu^2\overline{W}^2}{\overline{\epsilon}^2[\ln(J/J_0)]^2}\frac{\exp[-g(J)^2]}{\sqrt{4\pi}g(J)}, \tag{58}$$

with $g(J)\equiv g[r=\xi_0\ln(J_0/J)]$ [cf. Eq. (55)].

In Fig. 3, we plot the distribution $w(J)$ for four different parameter sets $(\overline{\epsilon},\overline{W},J_0)$ chosen such that the density of soliton-antisoliton pairs is fixed at $n_p=1/6000a^{-1}$ (with a the average carbon-carbon distance in *trans*polyacetylene). Our choice of parameters is summarized in Table I and will become clear in Sec. VI. Depending on the parameters, one observes two qualitatively very different behaviors: $w(J)$ either has a pronounced peak at $J^*\simeq J(r^*)$ [with $r^*=R^*d$ and R^* as in Eq. (35)] and tends to zero for $J\to 0$, or $w(J)$ diverges for small J. The distinction between these two behaviors is dominated by only one parameter combination

TABLE I. The four sets of parameters used in the numerical calculations for a fixed density of spin pairs, $n_p=1/6000a^{-1}$. The value for α as defined in Eq. (59) is obtained using the SSH parameter $\xi_0=7a$ for the correlation length.

$\overline{W}$ (μ/a)	$\overline{\epsilon}$ (μ^2/a)	J_0 (K)	α
0.038	0.010	400	0.5
0.055	0.014	130	0.75
0.070	0.017	72	1.0
0.100	0.023	39	1.5

$$\alpha=\frac{\overline{W}^2}{2\overline{\epsilon}}\xi_0. \tag{59}$$

In fact, Eq. (58) for $J\ll J^*$ yields

$$w(J)\propto\left(\frac{J_0}{J}\right)^{1-\alpha}, \tag{60}$$

which shows that the relative strength of the interchain interactions and the disorder determines whether $w(J)$ diverges ($\alpha<1$) or approaches zero ($\alpha>1$) for $J\to 0$.

The behavior of Eq. (60) agrees with Eq. (14) in Sec. III and can indeed be traced back to the fact that for large r the pair-size distribution is exponential

$$\overline{p}(r\gg r^*)\propto\exp\left(-\frac{\overline{W}^2 r}{2\overline{\epsilon}}\right)=\left(\frac{J_0}{J}\right)^{-\alpha}. \tag{61}$$

This exponential dependence can be understood as follows. For $r\gg r^*$, the energy of the string between soliton and antisoliton exceeds the kink creation energy: $\overline{W}r=WR\gg\mu$. Thus, the amplitude of the optimal fluctuation Eq. (34) is $h_R R\simeq WR$. The Gaussian weight $\exp[-Rh_R^2/(2\epsilon)]$ of this fluctuation is the exponential in Eq. (61). Similar arguments were used to explain the power-law dependence of the density of states in the fluctuating gap model of disordered systems.[26] The power-law dependence of $w(J)$ at small J gives rise to a characteristic low-temperature behavior of the magnetic susceptibility, as we will see in the next section.

VI. MAGNETIC SUSCEPTIBILITY OF *TRANS*POLYACETYLENE

In this section we consider *trans*polyacetylene as a disordered Peierls system and calculate its magnetic susceptibility due to disorder-induced soliton-antisoliton pairs as a function of temperature. The temperature dependence of the magnetic susceptibility is determined by the distribution of exchange constants Eq. (58). For temperatures T much larger than the typical singlet-triplet energy splitting J^*, almost all spin pairs are thermally excited. Thus, we have, essentially, $2n_p$

free spins, which give rise to a Curie susceptibility. Indeed, Eqs. (9) and (12) yield

$$\chi(T \gg J^*) \simeq \frac{1}{2} g^2 \mu_B^2 \beta \int_0^\infty dJ\, w(J) = \frac{1}{2} g^2 \mu_B^2 \frac{n_p}{T}, \quad (62)$$

where the density of soliton-antisoliton pairs n_p is given by Eq. (56). In the opposite limit, $T \ll J^*$, however, most of the spin pairs are in the singlet state and do not contribute to the magnetic susceptibility. Under these conditions Eqs. (12) and (58) yield

$$\chi(T \ll J^*) = C(T) \left(\frac{J_0}{T} \right)^{1-\alpha}, \quad (63)$$

with α as in Eq. (59) and logarithmic temperature corrections given by

$$C(T) \approx \frac{4 g^2 \mu_B^2}{9 J_0 \alpha} \left(\frac{n_p \xi_0}{\pi} \right)^{\frac{1}{2}} \frac{\mu^2}{\overline{\epsilon} \xi_0^2} \frac{\Gamma(1+\alpha) \mathrm{Li}_\alpha(-\frac{1}{3})}{[\ln(J_0/T)]^{5/2}} \quad (64)$$

[$\mathrm{Li}_\nu(z) = \Sigma_{k=1}^\infty z^k / k^\nu$ is the polylogarithm function]. The dominant factor in Eq. (63) is $(J_0/T)^{1-\alpha}$, which basically gives the density of spin pairs with singlet-triplet splitting $\sim T$ [cf. Eq. (60)].

We thus find that the low-temperature behavior of the magnetic susceptibility differs from the Curie law and is dictated by the relative strength α of interchain interactions and disorder. For $\alpha < 1$, the susceptibility diverges as $T \to 0$, while for $\alpha > 1$ it approaches zero.

A low-temperature ($T < 30$ K) deviation from Curie behavior has indeed been observed by Foot, Billingham, and Calvert in ESR experiments on Durham *trans*polyacetylene.[7] These authors already suggested pairing of spins as possible reason for this behavior. To see whether our model of spins associated with disorder-induced soliton-antisoliton pairs offers a microscopic explanation, we compared our result for $\chi(T)$ [numerically calculated from Eqs. (12) and (58)] to the experimental data. In our fit procedure there are, in principle, three free parameters: $\overline{W}$, $\overline{\epsilon}$, and J_0 (for the correlation length we take the SSH value $\xi_0 = 7a$). We require, however, that our parameters are also consistent with the total density of spin pairs, which is reported to be approximately $n_p = 1/6000 a^{-1}$.[4–7] This requirement imposes a relation between $\overline{W}$ and $\overline{\epsilon}$, reducing the number of free parameters to two.

In practice, we chose various values for α [Eq. (59)]. For each α value, $\overline{W}$ and $\overline{\epsilon}$ are uniquely determined by n_p, and J_0 is left as free parameter to fit the temperature dependence of the magnetic susceptibility. This procedure yielded the fits shown in Fig. 4, with parameter sets given in Table I. For convenience, we will refer to each parameter set by its α value. We note that our values for J_0 are much smaller than the value $J_0 = 4\Delta_0 \sim 10^4$ K, which is obtained within the SSH model.[17] We point out, however, that Coulomb interactions result in a reduction of the value for J_0.

The important point is now that, while all four parameter sets give rise to reasonable fits of the experimental data, they predict totally different behaviors for $T \lesssim 5$ K, where experiments have not been performed. This is shown in Fig. 5, where we extend the four theoretical fits to 1 K. The qualitative differences in the low-temperature behavior, dictated by the value of α, are clearly visible below 5 K. This suggests that extending the experiments to lower temperatures may yield more information on the relative strength of interchain interactions and disorder in *trans*polyacetylene.

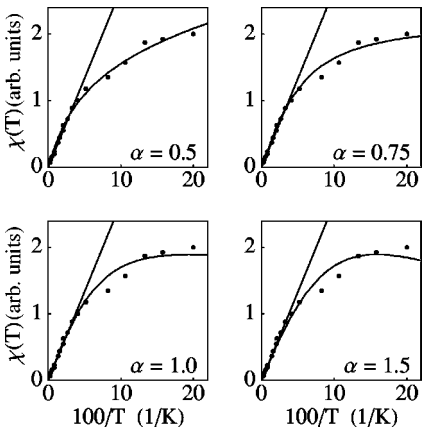

FIG. 4. Fits of our theory (solid curve) to the experimental data (dots) for the magnetic susceptibility of Durham *trans*polyacetylene obtained in Ref. 7. The four parameter sets given in Table I were used to fit the same experimental data points (see text for details). The deviation from Curie behavior (straight line) below $T = 30$ K is clearly seen and reasonably reproduced by each fit down to $T = 5$ K, below which experimental data are not available.

We conclude this section by noting that, within the context of our model, it is possible to determine the strength of the interchain interactions and the disorder independent of the fitting parameter J_0. For this purpose, the density n_p of soliton-antisoliton pairs is to be obtained experimentally from the Curie tail of the magnetic susceptibility, while for the same sample α is to be determined from the asymptotic zero-temperature behavior of the magnetic susceptibility. Then, using Eqs. (56) and (59), the strength of the interchain interactions,

$$\overline{W} \approx 4\alpha \frac{\mu}{\xi_0} \left[\ln\left(\frac{4\alpha}{n_p \xi_0} \right) \right]^{-1}, \quad (65)$$

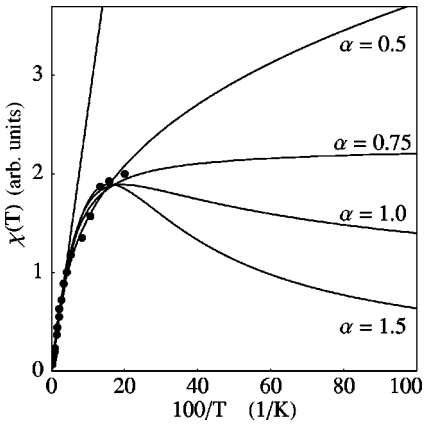

FIG. 5. As Fig. 4, but now the four theoretical curves are shown down to $T = 1$ K. It is clearly observed that different values of α (the relative strength of disorder and interchain interactions) lead to qualitatively different low-T (< 5 K) behavior of the magnetic susceptiblity.

and the disorder strength,

$$\overline{\epsilon} \approx 8\alpha \frac{\mu^2}{\xi_0}\left[\ln\left(\frac{4\alpha}{n_p \xi_0}\right)\right]^{-2}, \tag{66}$$

can be calculated as a function of n_p and α. For typical values of the density n_p the logarithmic factor depends only weakly on $\alpha \sim O(1)$ and can be approximated by a numerical constant. If $n_p = 1/6000a^{-1}$ and choosing again the SSH parameter $\xi_0 = 7a$, one obtains $\overline{W} \approx 0.07\alpha\mu/a$ and $\overline{\epsilon} \approx 0.02\alpha\mu^2/a$. It is important to realize that Eqs. (65) and (66) do not depend on the maximal exchange constant J_0, which may be used as a fitting parameter for temperatures around the typical exchange J^*.

VII. CONCLUDING REMARKS

To summarize, we have calculated the magnetic susceptibility of quasi-one-dimensional Peierls systems with a doubly degenerate ground state. We have related the temperature-dependent part of the susceptibility to the presence of neutral solitons and antisolitons with spin $\frac{1}{2}$ induced by disorder in the electron hopping amplitudes along the chain. We have assumed the interchain interactions to be sufficiently strong to bind the disorder-induced solitons and antisolitons into pairs and thus establish long-range bond order in the system. Using a mapping on the random-field Ising model, we have calculated the distribution of the soliton-antisoliton pair size. This allowed us to obtain the distribution of exchange constants describing the interaction between the spins of the soliton and the antisoliton within one pair. Both distributions strongly depend on the relative strength α of the disorder and the interchain interactions. As a result, the magnetic susceptibility deviates from the Curie law: below $T = J^*$, where J^* is the most probable value of the exchange constant, the magnetic susceptibility behaves as $(1/T)^{1-\alpha}$.

Our results explain the deviation from Curie behavior observed in Durham *trans*polyacetylene,[7] though from the experimental data it is difficult to find unambiguously the values of α and J^* for this conjugated polymer. It is, therefore, important to extend the measurements to lower temperatures, where the temperature dependence of the magnetic susceptibility is extremely sensitive to the choice of parameters.

Our theory is only applicable when the low-temperature behavior of the susceptibility is an intrinsic property of the material and is not governed by spins of impurities. The latter situation may, in fact, be realized in Shirakawa *trans*polyacetylene, which shows Curie behavior down to $T = 1.5$ K.[27] Furthermore, we assumed the existence of long-range order in the system. Whether this is the case in *trans*polyacetylene is an open question. It would, therefore, be interesting to extend our studies to the case without long-range order. At the same time, however, it should be noted that in substituted polyacetylenes, the degeneracy of the two dimerized configurations may be lifted. This leads to an extra (intrachain) source of soliton-antisoliton confinement[28] and favors long-range bond order. Our theory may be applied to these substituted polymers by simply adding to the interchain interaction per bond (Wa), the energy difference per bond between the two dimerized configurations. As this energy difference may be controlled by varying the substitutions, this opens interesting possibilities to study disorder-induced solitons in more detail.

We finally mention that in the ordered phase, the disorder-induced soliton-antisoliton pairs show up in the x-ray spectrum as a broad incoherent peak associated with each sharp elastic peak arising from the bond length alternation. Our result for the pair-size distribution allows one to calculate the shape of this incoherent peak: it simply is the Fourier transform squared of the connected correlator Eq. (51). Thus, one immediately finds that the peak width is $\sim 1/r^* \approx \overline{W}/\mu$. It should be kept in mind, however, that this calculation does not account for other broadening mechanisms, e.g., those due to the complicated morphology of polyacetylene samples.

ACKNOWLEDGMENT

This work is part of the research program of the Stichting Fundamenteel Onderzoek der Materie (FOM), which is financially supported by the Nederlandse Organisatie voor Wetenschappelijk Onderzoek (NWO).

[1] M.V. Mostovoy, M.T. Figge, and J. Knoester, Europhys. Lett. **38**, 687 (1997).
[2] M.V. Mostovoy, M.T. Figge, and J. Knoester, Phys. Rev. B **57**, 2861 (1998).
[3] S.N. Yaliraki and R.J. Silbey, J. Chem. Phys. **104**, 1245 (1996).
[4] H. Shirakawa, I. Ito, and S. Ikeda, Makromol. Chem. **179**, 1565 (1978).
[5] I.B. Goldberg, H.R. Crowe, P.R. Newman, A.J. Heeger, and A.G. MacDiarmid, J. Chem. Phys. **70**, 1132 (1979).
[6] B.R. Weinberger, E. Ehrenfreund, A. Pron, A.J. Heeger, and A.G. MacDiarmid, J. Chem. Phys. **72**, 4749 (1980).
[7] P.J.S. Foot, N.C. Billingham, and P.D. Calvert, Synth. Met. **16**, 265 (1986).
[8] W.P. Su, J.R. Schrieffer, and A.J. Heeger, Phys. Rev. Lett. **42**, 1698 (1979).
[9] B.R. Weinberger, C.B. Roxlo, S. Etemad, G.L. Baker, and J. Orenstein, Phys. Rev. Lett. **53**, 86 (1984).
[10] D. Baeriswyl, D.K. Campbell, and S. Mazumdar, Phys. Rev. Lett. **56**, 1509 (1986); Synth. Met. **17**, 197 (1987).
[11] Z. Vardeny and J. Tauc, Phys. Rev. Lett. **54**, 1844 (1985); **56**, 1510 (1986).
[12] M.V. Mostovoy and J. Knoester, Phys. Rev. B **53**, 12 057 (1996): **54**, 9784 (1996).
[13] J.H.F. Martens, K. Pichler, E.A. Marseglia, R.H. Friend, H. Cramail, E. Khosravi, D. Parker, and W.J. Feast, Polymer **35**, 403 (1994), and references therein.
[14] D.C. Bott, C.S. Brown, J.N. Winter, and J. Baker, Polymer **28**, 601 (1987).
[15] H. Kahlert, O. Leitner, and G. Leising, Synth. Met. **17**, 467 (1987).
[16] G. Perego, G. Lugli, U. Pedretti, and M. Cesari, Makromol. Chem. **189**, 2657 (1988).

[17] Y.R. Lin-Liu and K. Maki, Phys. Rev. B **22**, 5754 (1980).
[18] M.T. Figge, M.V. Mostovoy, and J. Knoester, Phys. Rev. B **58**, 2626 (1998).
[19] S. Kivelson and D.E. Heim, Phys. Rev. B **26**, 4278 (1982).
[20] D.K. Campbell, T.A. deGrand, and S. Mazumdar, Phys. Rev. Lett. **52**, 1717 (1984).
[21] J. Mertsching (unpublished).
[22] D. Baeriswyl and K. Maki, Phys. Rev. B **28**, 2068 (1983).
[23] Y. Imry and S. Ma, Phys. Rev. Lett. **35**, 1399 (1975).
[24] W.G. Clark, L.C. Tippie, G. Frossati, and H. Godfrin, J. Phys. (France) **39**, C6-365 (1978); W.G. Clark and L.C. Tippie, Phys. Rev. B **20**, 2914 (1979).
[25] I.M. Lifshitz, Zh. Éksp. Teor. Fiz. **53**, 743 (1968) [Sov. Phys. JETP **26**, 462 (1968)].
[26] M.V. Mostovoy and J. Knoester, Phys. Lett. A **235**, 535 (1997).
[27] M. Schwoerer, U. Lauterbach, W. Müller, and G. Wegner, Chem. Phys. Lett. **69**, 359 (1980).
[28] S. Takeuchi, T. Masuda, and T. Kobayashi, J. Chem. Phys. **105**, 2859 (1996).